Fuel Governor Augmented Control of Recompression HCCI Combustion During Large Load Transients

Shyam Jade, Erik Hellström, Li Jiang, Anna G. Stefanopoulou

***Abstract*— A control strategy designed to track desired combustion phasing for a homogeneous charge compression ignition (HCCI) engine during large load transitions is presented in this work. Three inputs are controlled, namely valve timings, fuel injection amount and fuel injection timing. The valve and fuel injection timings are manipulated to track combustion phasing using a mid-ranging control strategy. A fuel governor is then added on to the compensated system to modify the fuel injection amount by enforcing pointwise-in-time actuator constraints.**

The fuel governor is shown to improve the transient response of combustion phasing and load during large load transitions, when the possibility of future constraint violations exists. The use of the fuel governor during large load reductions can prevent engine misfire. Moreover, the fuel governor strategy simplifies the overall controller design by decoupling the phasing controller from the constraint enforcing mechanism. System complexity is reduced by approximating the nonlinear fuel governor as a set of linear algebraic expressions. This is solved with very little computational overhead and without incurring a significant loss in performance, as presented in simulations.

I. Introduction

The goal of this work is to design a control strategy that can track combustion phasing in a recompression homogeneous charge compression ignition (HCCI) engine, especially during large load transitions. Auto-ignition timing control in HCCI combustion requires careful regulation of the temperature, pressure and composition of the pre-combustion cylinder charge. In recompression HCCI, actuators indirectly influence these charge properties through the trapping of hot residual gases. Large load transients can often lead to actuator saturation, in which case the controller authority is lost.

Solutions to this problem using optimal control schemes have been proposed, see for example [1], [2]. However, these often involve the on-line solving of a nonlinear optimization problem where the stabilization, tracking and actuator constraint fulfillment requirements have to be satisfied simultaneously. This problem is simplified through the implementation of the fuel governor concept, which separates the closed loop design from the constraint enforcement requirement [3]. This reduces computation time compared to higher-dimensional optimal control schemes, at the cost of reduced flexibility in shaping the transient response.

Fig. 1 shows an overview of the methodology used in this work. Load requirements are converted into desired fuel mass commands (m_f^{des}). The effects of fuel mass changes on combustion phasing are to be rejected. A controller actuating valve timings and fuel injection timing is implemented to track desired combustion phasing (θ_{CA50}^{ref}). The fuel governor is then added on to the controller-augmented nonlinear system to improve transient responses during large load transitions. It works by attenuating the desired fuel amount change when the possibility of future actuator constraint violations exists. Although the current application deals with actuator constraint enforcement alone, the methodology can be extended to consider state-related pointwise-in-time constraints as well. For example, in HCCI combustion control additional constraints on pressure rise rates, air-to-fuel ratios, emissions, etc. can be considered.

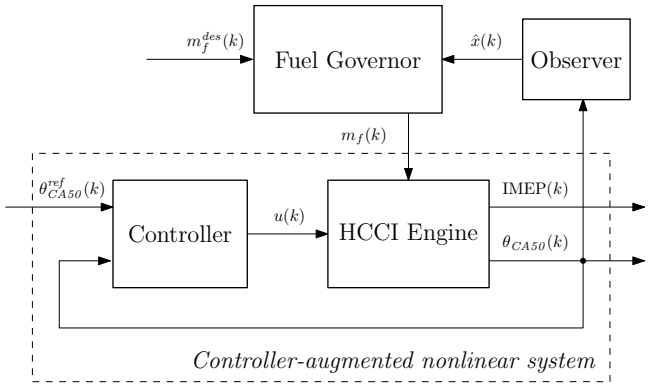

Fig. 1. Fuel governor added on the controller-augmented nonlinear plant

The fuel governor constraint-enforcement mechanism has been applied to other physical systems such as fuel cells [4]–[6] and electric power generation [7], [8]. Theoretical results discussing the stability, performance, and implementation of reference governors in linear and non-linear systems have been developed in literature, see for example [3], [9]–[14].

This paper is organized as follows. Section II introduces the HCCI combustion model, and discusses actuator dynamics and constraints. Section III deals with the design of the closed loop system, as well as feedback gain selection. Section IV describes the design of the nonlinear fuel governor. This is simplified into a set of analytically-derived linear equations, resulting in significant computation time improvements. Finally, simulation results are presented in Sec. V.

II. HCCI engine model

In recompression HCCI [15], the exhaust valve is closed early and the intake valve is opened late, resulting in a negative valve overlap (NVO). This can be seen in Fig. 2, which shows a typical in-cylinder pressure trace for a recompression-based HCCI engine. During this phase, the trapped residual

S. Jade (sjade@umich.edu), E. Hellström (erikhe@umich.edu) and A. Stefanopoulou (annastef@umich.edu) are with the Department of Mechanical Engineering in the University of Michigan, Ann Arbor. L. Jiang (li.jiang@us.bosch.com) is with Robert Bosch LLC, Farmington Hills.

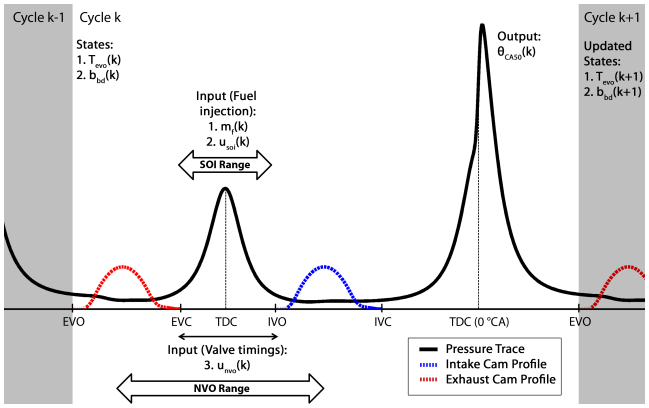

Fig. 2. Typical HCCI in-cylinder pressure trace

gases undergo a secondary compression and expansion. Manipulating NVO changes the mass fraction of hot residuals trapped in the cylinder. This affects the temperature of the pre-combustion gas mixture, which significantly influences the thermally-dominant HCCI combustion dynamics. All the fuel is injected in a single fuel injection, the timing of which can be varied within the recompression region. Variable fuel injection timing shows promising results in HCCI combustion phasing control [16].

A. Model states, inputs and outputs

The zero dimensional, control-oriented model for recompression HCCI combustion developed in [17] is used in this work. The combustion model has two discrete states – (i) the temperature of the gases at exhaust valve opening (T_{evo}), and (ii) the burned gas fraction of the blowdown gases (b_{bd}). These represent thermal and composition dynamics respectively. The burned gas fraction is the mass fraction of the combustion products excluding excess air. For further details, refer [17].

The actuator inputs considered for control are the negative valve overlap (NVO), start of fuel injection (SOI), and mass of fuel injected (m_f). Valve timings are controlled by a cam phasing actuator with fixed cam profiles. Here the exhaust cam position is varied, while the intake cam position is fixed.

The primary performance output of the model is combustion phasing. This is quantified by the location of θ_{CA10}, θ_{CA50} and θ_{CA90}, which are the engine crank angles at which 10%, 50% and 90% respectively of the total heat release occur. The work output, represented by the indicated mean effective pressure (IMEP), is seen to be a very strong function of the mass of fuel injected. In this work, load transitions will henceforth be represented by fuel mass changes.

The relative locations of the inputs, outputs and states can be seen in Fig. 2. Each engine cycle ends at exhaust valve opening (EVO). The combustion top dead center (TDC) is considered to be the 0° CA location. In this work, all results are presented at a fixed engine speed of 2000 RPM.

B. Actuator dynamics

The NVO and SOI actuators differ in their ranges, the relative magnitude of their authorities, and their bandwidth.

TABLE I
LINEARIZATION OPERATION POINT

Quantity (α)	Nominal operating point $(\bar{\alpha})$	Normalization constant $(\tilde{\alpha})$	Units
NVO	180	25	°CA
m_f	9	3	mg/cycle
SOI	350	50	°CA bTDC
θ_{CA50}	6.22	-	°CA aTDC
IMEP	2.42	-	bar
T_{evo}	780	150	K
b_{bd}	0.7425	0.25	-

The NVO actuator has the larger range, as can be seen in Fig. 2. It also has much greater authority. As discussed earlier, varying NVO can significantly affect the trapped residual gas fraction, which in turn has an important influence on the thermally-dominant HCCI combustion dynamics. This can be seen from the coefficients of the normalized linear model given later in (5). However, the hydraulic cam phasing actuator for valve timings considered is slow. This is represented by the low maximum actuator rate (see Δu_{nvo} in (3)). In contrast, there is complete flexibility to realize any fuel injection timing within the allowable range. This results in a larger bandwidth for the SOI actuator, making it attractive for cycle-to-cycle control.

C. Combustion model system equations

The nonlinear system equations for the combustion model are given by

$$\begin{aligned} x(k+1) &= f\left(x(k), u(k), m_f(k)\right) \\ \theta_{CA50}(k) &= g\left(x(k), u(k), m_f(k)\right) \\ x = [b_{bd}, T_{evo}]^T \quad & u = [u_{nvo}, u_{soi}]^T \end{aligned} \tag{1}$$

where x is the state vector, u is the vector of inputs, and m_f is the fuel mass. Further, u is constrained as follows.

$$\begin{aligned} u_{soi}^{min} \le u_{soi} \le u_{soi}^{max} \\ u_{nvo}^{min} \le u_{nvo} \le u_{nvo}^{max} \\ |u_{nvo}(k) - u_{nvo}(k-1)| < \Delta u_{nvo} \end{aligned} \tag{2}$$

The constants are hardware dependent. Here the following typical values are considered:

$$\begin{aligned} u_{soi}^{min} = 300^\circ \text{ CA bTDC}, \quad u_{soi}^{max} = 400^\circ \text{ CA bTDC}, \\ u_{nvo}^{min} = 150^\circ \text{ CA}, \quad u_{nvo}^{max} = 225^\circ \text{ CA}, \\ \Delta u_{nvo} = 4^\circ \text{ CA/cycle at 2000 RPM}. \end{aligned} \tag{3}$$

The nonlinear system of equations in (1) is linearized about the nominal operating point specified in Table I. The states and inputs in (4) and (5) are normalized by their typical maximum ranges about the operating point. The normalized value of any quantity α is given by $\tilde{\alpha} = \frac{\alpha - \bar{\alpha}}{\Delta\alpha}$ where $\tilde{\alpha}$, $\bar{\alpha}$ and $\Delta\alpha$ are the normalized value, nominal operating point

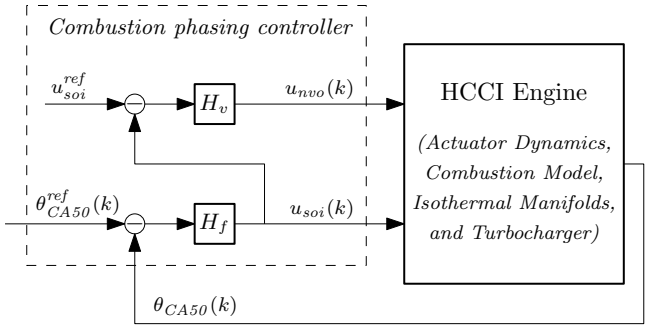

Fig. 3. TISO controller for tracking combustion phasing

and typical maximum range of α respectively.

$$\begin{aligned}\tilde{x}(k+1) &= A\tilde{x}(k) + B\tilde{u}(k) + B_f\tilde{m}_f(k)\\ \theta_{CA50}(k) - \bar{\theta}_{CA50}(k) &= C\tilde{x}(k) + D\tilde{u}(k) + D_f\tilde{m}_f(k)\\ \tilde{x} = \left[\tilde{b}_{bd}, \tilde{T}_{evo}\right]^T \quad \tilde{u} &= [\tilde{u}_{nvo}, \tilde{u}_{soi}]^T\\ B = [B_{nvo}, B_{soi}] \quad D &= [D_{nvo}, D_{soi}]\end{aligned} \tag{4}$$

where

$$\begin{aligned}A = \begin{bmatrix} 0.535 & -0.070 \\ -0.095 & 0.357 \end{bmatrix} \quad B &= \begin{bmatrix} 0.513 & 0.027 \\ 0.378 & 0.104 \end{bmatrix}\\ B_f = [0.476, 0.637]^T \quad C &= [0, -9.852]\\ D = [-12.724, -3.057] \quad D_f &= -0.454\end{aligned} \tag{5}$$

The linearized model is used to develop the analytically-derived linear fuel governor in Sec. IV-C, and to design the observer in Sec. IV-D. Fuel amount changes are seen to have a significant influence on the states, and consequently combustion phasing. This makes rejecting the effect of fuel on combustion phasing an important design requirement.

III. Combustion phasing controller

The two-input single-output (TISO) control strategy outlined in Fig. 3 tracks the desired reference signal (θ_{CA50}^{ref}), while rejecting the effects of the fuel mass signal (m_f). The combustion phasing output of the system is θ_{CA50}, while the two inputs are u_{nvo} and u_{soi}. The reference SOI value (u_{soi}^{ref}) is fixed at 350° CA bTDC, about which the SOI actuator has adequate control authority in both directions. A similar control strategy is seen in [18].

A. Feedback loop

The feedback loop consists of two PI controllers arranged in a mid-ranging control configuration. Mid-ranging is a TISO control technique often used in process control [19]. It is useful in situations where one actuator provides the required range but has poor resolution, while the other actuator is fast but saturates easily. To provide high resolution over the entire operating range, the slow actuator returns the fast actuator to its reference set point at steady state.

In this implementation, the θ_{CA50} tracking error signal drives a PI controller (H_f in Fig. 3) that controls the fuel injection timing, which is the fast but easily saturated actuator. The slower NVO signal that provides the required capacity is used to mid-range the SOI actuator back towards its nominal reference value. This is accomplished using another PI controller (H_v in Fig. 3) driven by the SOI tracking error. Integrator anti-windup mechanisms are implemented on both integrators, improving performance during transients caused by large fuel transitions.

To summarize, the SOI and NVO control signals are given by (6) and (7), where H_v and H_f are respectively the NVO and SOI PI feedback controllers with antiwindup.

$$u_{soi} = H_f(\theta_{CA50} - \theta_{CA50}^{ref}) \tag{6}$$

$$u_{nvo} = H_v(u_{soi} - u_{soi}^{ref}) \tag{7}$$

B. Optimization of feedback gains

An nonlinear least-squares optimization was carried out on the controller-augmented plant with actuator dynamics to determine the optimal values of the feedback controller gains in (6) and (7). The four parameters that are optimized are the two proportional gains and two integral gains in H_v and H_f. A typical input target excitation cycle of θ_{CA50}^{ref} steps and large fuel steps and ramps is used in the optimization process. The ability of the controller to track θ_{CA50}^{ref} while rejecting the effect of large fuel transients is evaluated using the optimization cost function considered in (8). Here α is an optimization weight that represents a trade-off between tracking error and controller effort.

$$J = \sum \left(\theta_{CA50} - \theta_{CA50}^{ref}\right)^2 + \alpha \sum \left(u_{soi} - u_{soi}^{ref}\right)^2 \tag{8}$$

Alternatively, the linearized plant model can be be used to tune midranging controllers, see for example [20], [21].

IV. Fuel governor

The fuel governor is added on to the controller-augmented nonlinear system to improve transient performance by enforcing actuator constraints, as seen in Fig. 1. It works by slowing down the fuel amount signal if future constraint violations are predicted. As opposed to passively filtering the fuel amount signal, the model-based fuel governor only modifies large fuel transitions that will violate actuator constraints. Further, IMEP response is maintained by avoiding excessive slowing down of the fuel signal.

The nonlinear fuel governor is designed in Sec. IV-A. The prediction model used in the governor is discussed in Sec. IV-B. Computation times are significantly reduced by by representing the fuel governor as a set of linear algebraic expressions in Sec. IV-C. An observer is designed to estimate combustion states in Sec. IV-D. Finally, Sec. IV-E discusses errors in the fuel governor predictions.

A. Nonlinear fuel governor design

The fuel governor utilizes the receding horizon principle to satisfy actuator constraints. Similar to [4], a bisectional search is carried out on the desired change in fuel amount. This involves the optimization of a single parameter, namely β in (9). Ideally β is set to 1, in which case the fuel governor

has no effect, and the desired fuel step is applied unmodified to the closed loop system.

$$m_f(k) = m_f(k-1) + \beta \cdot (m_f^{des}(k) - m_f(k-1)) \quad (9)$$

At every time step, a model of the closed loop system is simulated over a fixed future interval with the fuel level maintained at $m_f(k)$ calculated in (9). The system is initialized using the combustion model states estimated by the observer. If constraint violations are detected, the parameter β is reduced, and the simulation is reinitialized. If all constraints are satisfied, β is increased until the optimal value of $\beta \in [0, 1]$ is obtained, subject to a predetermined tolerance for convergence of β. In addition to constraint satisfaction, the bisectional search reduces the tracking error between desired and actual fuel levels. In this work, a time horizon of 4 cycles, and a tolerance of 0.1 is used. These values were tuned to balance prediction accuracy and speed.

B. Prediction model for nonlinear fuel governor

The fuel governor design requires a controller-augmented combustion model to predict future actuator positions. To account for the effects of the manifolds, the intake and exhaust manifold pressures are assumed to be available as measurements and are maintained constant over the time horizon considered. The error introduced by this assumption is small due to the short horizon length, and the relatively slow manifold dynamics. Estimation of exhaust manifold pressure in turbocharged engines is discussed in literature, see for example [22], and could be incorporated in the future.

C. Analytically-derived linear fuel governor

The linearized closed-loop model can be used to analytically derive expressions for constraint violation. The online portion of the fuel governor is then reduced to evaluating a set of simple algebraic equations with pre-computed scalar coefficients. This significantly reduces the computation time required, at a slight cost of fuel governor performance.

The linearized combustion model developed in Sec. II-C is augmented with the controller developed in Sec. III (without the integrator anti-windup). The state space representation of this closed loop system between inputs as mass of fuel (m_f) and θ_{CA50}^{ref} and outputs as NVO and SOI is given by (10).

$$\begin{aligned} x_{CL}(k+1) &= A_{CL}x_{CL}(k) + B_f m_f(k) + B_{ref}\theta_{CA50}^{ref}(k) \\ u_{nvo}(k) &= C_1 x_{CL}(k) + D_{f,1} m_f(k) + D_{ref,1}\theta_{CA50}^{ref}(k) \\ u_{soi}(k) &= C_2 x_{CL}(k) + D_{f,2} m_f(k) + D_{ref,2}\theta_{CA50}^{ref}(k) \end{aligned} \quad (10)$$

Given a desired mass of fuel to be injected (m_f^{des}), the fuel governor checks if it is permissible in the following manner. The initial state $x_{CL}(0)$ of the closed loop system is estimated by the observer. Assuming that the inputs m_f and θ_{CA50}^{ref} stay constant over the time horizon $N \geq 1$ considered, algebraic closed form solutions can be derived for the evolution of NVO and SOI over future cycles $1, \ldots, N$. For example, NVO n cycles into the simulation is given by (11).

$$\begin{aligned} u_{nvo}(n) &= C_1 A_{CL}^n x_{CL}(0) \\ &+ \left(C_1 \left(A_{CL}^{(n-1)} + \ldots + A_{CL} + I \right) B_{ref} + D_{ref,1} \right) \theta_{CA50}^{ref} \\ &+ \left(C_1 \left(A_{CL}^{(n-1)} + \ldots + A_{CL} + I \right) B_f + D_{f,1} \right) m_f \end{aligned} \quad (11)$$

This is then inverted to give (12), where m_f is expressed as a linear function of $u_{nvo}(n)$. Here γ_x are fixed scalars that can be calculated offline.

$$m_f(n) = \gamma_1(n) u_{nvo}(n) + \gamma_2(n, x_{CL}(0), \theta_{CA50}^{ref}) \quad (12)$$

Let $S_{nvo}^{sat}(n)$ be the range of fuel amounts permissible for the NVO saturation constraint to be satisfied in cycle n. Since (12) is linear, this can be characterized by plugging in the actuator limits u_{nvo}^{max} and u_{nvo}^{min} defined in (2).

$$\begin{aligned} m_f^{min}(n) &= \gamma_1(n) u_{nvo}^{max} + \gamma_2(n, x_{CL}(0), \theta_{CA50}^{ref}) \\ m_f^{max}(n) &= \gamma_1(n) u_{nvo}^{min} + \gamma_2(n, x_{CL}(0), \theta_{CA50}^{ref}) \\ S_{nvo}^{sat}(n) &= \left[m_f^{min}(n), m_f^{max}(n) \right] \end{aligned} \quad (13)$$

This process is repeated over the time horizon N and a family of subsets $S_{nvo}^{sat}(k),\ k \in \{1, \ldots, N\}$ is generated. The intersection of all of these subsets gives $\overline{S_{nvo}^{sat}}$, which is the permissible fuel range for the NVO saturation constraint to be satisfied over the entire time horizon.

$$\overline{S_{nvo}^{sat}} = \bigcap_{k=\{1,\ldots n\}} S_{nvo}^{sat}(k). \quad (14)$$

The other actuator constraints in (2) can be handled similarly to obtain $\overline{S_{nvo}^{rate}}$ and $\overline{S_{soi}^{sat}}$, which are the permissible fuel ranges for the NVO rate constraint and the SOI saturation constraint respectively to be satisfied over the entire time horizon. The overall minimum (m_f^{min}) and maximum (m_f^{max}) fuel masses that satisfy all constraints are given in (15). Finally the fuel mass injected $(m_f(k))$ is given by (16).

$$\left[m_f^{min}, m_f^{max} \right] = \overline{S_{nvo}^{sat}} \cap \overline{S_{nvo}^{rate}} \cap \overline{S_{soi}^{sat}} \quad (15)$$

$$m_f(k) = \begin{cases} m_f^{min} & \text{if } m_f^{des}(k) < m_f^{min}, \\ m_f^{max} & \text{if } m_f^{des}(k) > m_f^{max} \\ m_f^{des}(k) & \text{otherwise.} \end{cases} \quad (16)$$

The coefficients in all of these equations are known and can be calculated offline. The fuel governor is reduced to solving a set of algebraic equations with known coefficients.

1) Performance comparison: Table II demonstrates the significant reduction in computation time when the constraints are converted to algebraic expressions. In each case a test cycle of θ_{CA50}^{ref} steps and large fuel steps which lasts for one hundred seconds is simulated. As can be seen, the analytically-derived linear fuel governor runs over an order of magnitude faster than the nonlinear fuel governor, while introducing very little overhead compared to the no fuel governor case.

2) Alternative schemes: Alternative schemes to speed up reference governor computation times are discussed in literature, see for example [12], [23].

TABLE II

RELATIVE COMPUTATION TIME COMPARISON

Scheme	Normalized computation time
No Fuel Governor	100%
Linear Fuel Governor	102%
Nonlinear Fuel Governor	3490%

D. Observer for discrete combustion states

Both the nonlinear fuel governor and the analytically-derived linear fuel governor require the estimation of the discrete combustion states. A Luenberger observer is designed for the combustion model states using the plant linearization considered in Sec. II-C.

E. Errors in fuel governor predictions

Some of the design choices made to reduce complexity increase errors in the actuator position predictions. The simplified prediction model developed in Sec. IV-B does not fully represent the dynamics of the engine. The analytically-derived linear fuel governor developed in Sec. IV-C uses the combustion model linearized at a single operation point as the basis for its predictions. The nonlinearities inherent in the system cause increased errors in the state estimated by the linear observer as one moves away from the nominal operating point. The fuel governor design is made more conservative to deal with all of these modeling errors, and to ensure that the actuator constraints are not violated.

V. RESULTS

The closed loop system designed in Sec. III exhibits good disturbance-tolerant tracking performance for small fuel steps, as seen in the plots on the left of Fig. 4. However, large fuel steps often result in actuator constraint violations. In these cases, the system is governed by open-loop dynamics and the controller's ability to shape the transient response of the system is lost. The plots on the right of Fig. 4 show that the engine can even misfire for large fuel steps. The large fuel step chosen in the figure spans the range of fuel amounts for which the combustion model is validated.

This unacceptable performance during large fuel steps is improved in Fig. 5 through the use of fuel governors. The three control strategies compared in this figure are:

1) Nonlinear fuel governor with observer, from Sec. IV-A.
2) Linear fuel governor, from Sec. IV-C.
3) Closed loop system with no fuel governor, from Sec. III.

It is seen that the use of fuel governors improves θ_{CA50} tracking, while maintaining IMEP settling times and reducing IMEP overshoots. There is a slight reduction in performance when using the analytically-derived linear fuel governor. However, the significant reduction in computational time demonstrated in Tab. II makes this scheme an attractive choice. The reduction of the large θ_{CA50} overshoots during load steps is important. Too large an overshoot when the load steps down can lead to the engine misfiring. Similarly too large an overshoot when the load increases can lead to excessive

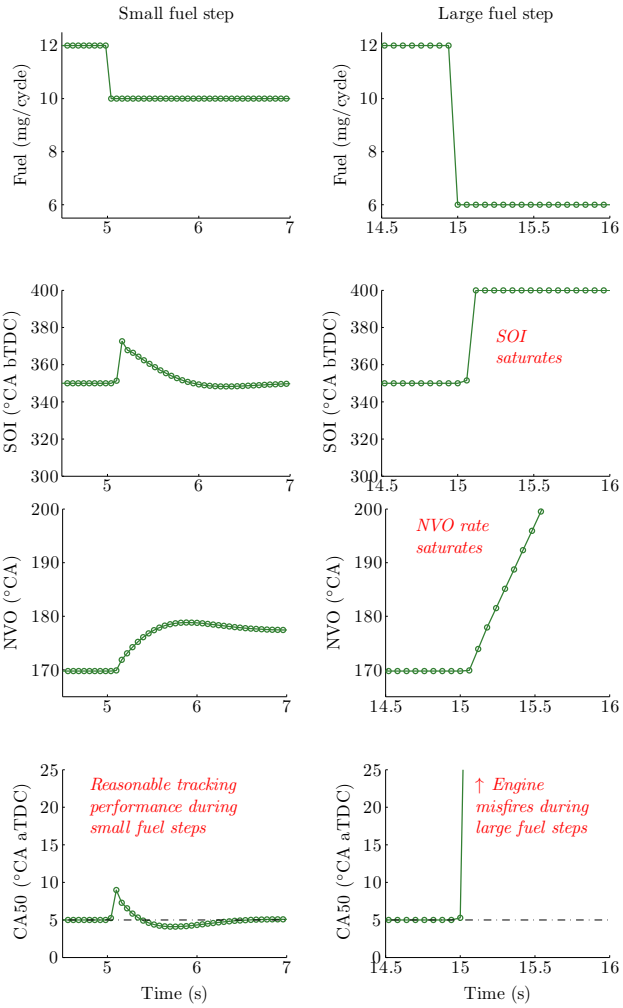

Fig. 4. Tracking performance of the system without fuel governor. Simulation results for small and large fuel steps.

pressure rise rates. Combustion phasing tracking results in the absence of any fuel changes, or for small fuel transitions which do not cause the actuators to saturate, are exactly the same for all schemes.

VI. CONCLUSIONS

Large load transitions in HCCI engines can lead to excessive pressure rise rates or engine misfires. The fuel governor methodology provides a systematic way to separate the combustion phasing controller design from the actuator constraint enforcement task. The governor can be considered to be a model-based variable bandwidth filter. It optimizes the rate at which the fuel command is slowed down, while ensuring that actuator authority is not lost. This implementation can be extended to handle state-based constraints, such as restrictions on pressure rise rates and emissions.

The fuel governor approach optimizes a single variable, and so is intrinsically less complex than higher-dimensional optimal control schemes. Complexity can be further significantly reduced by approximating the nonlinear fuel governor as a set of linear algebraic equations with pre-determined

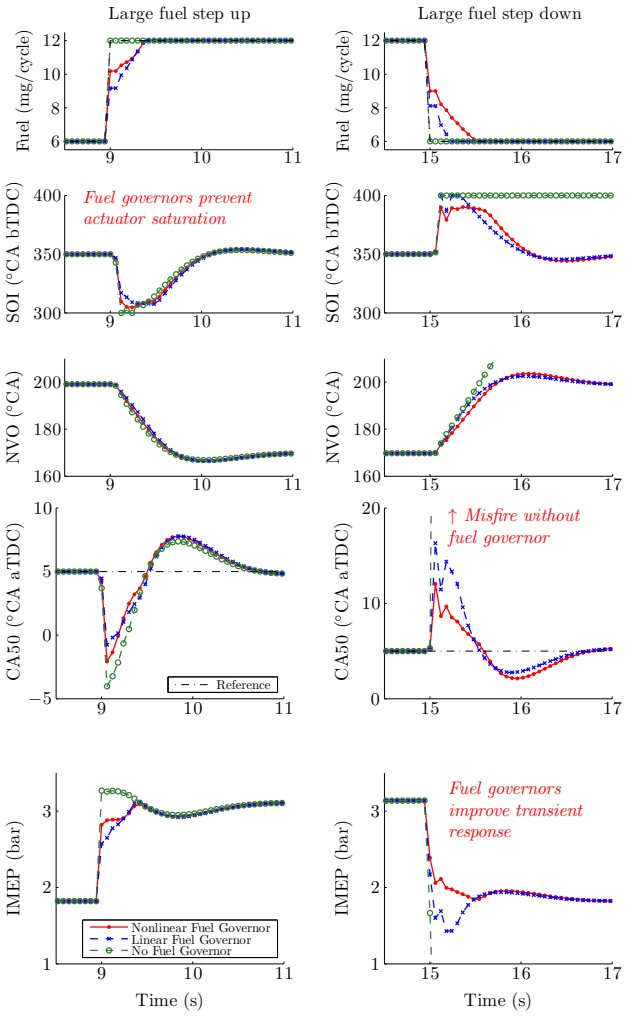

Fig. 5. Combustion phasing regulation performance during large load steps up and down.

coefficients. This design has to be made more conservative to prevent constraint violation.

Promising simulation results are obtained for both the nonlinear fuel governor and the analytically-derived linear fuel governor. The fuel governors improve θ_{CA50} tracking performance and IMEP transient response during large load transitions. During large load reductions, the fuel governors are able to prevent engine misfires. Experimental validation of this approach is underway.

Acknowledgments[1]

This material is supported by the Department of Energy (National Energy Technology Laboratory, DE-EE0003533) as part of the ACCESS project consortium under the direction of Principal Investigator Hakan Yilmaz, Robert Bosch, LLC.

[1]Disclaimer: This report was prepared as an account of work sponsored by an agency of the United States Government. Neither the United States Government nor any agency thereof, nor any of their employees, makes any warranty, express or implied, or assumes any legal liability or responsibility for the accuracy, completeness, or usefulness of any information, apparatus, product, or process disclosed, or represents that its use would not infringe privately owned rights. Reference herein to any specific commercial product, process, or service by trade name, trademark, manufacturer, or otherwise does not necessarily constitute or imply its endorsement, recommendation, or favoring by the United States Government or any agency thereof. The views and opinions of authors expressed herein do not necessarily state or reflect those of the United States Government or any agency thereof.

References

[1] J. Bengtsson, P. Strandh, R. Johansson, P. Tunestal, and B. Johansson, "Model predictive control of Homogeneous Charge Compression Ignition (HCCI) engine dynamics," *IEEE International Conference on Control Applications*, pp. 1675–1680, 2006.

[2] C.-J. Chiang and C.-L. Chen, "Constrained control of Homogeneous Charge Compression Ignition (HCCI) engines," *5th IEEE Conference on Industrial Electronics and Applications*, pp. 2181–2186, 2010.

[3] A. Bemporad, "Reference governor for constrained nonlinear systems," *IEEE Trans. Autom. Control*, vol. 43, no. 3, pp. 415–419, 1998.

[4] J. Sun and I. Kolmanovsky, "Load governor for fuel cell oxygen starvation protection: a robust nonlinear reference governor approach," *IEEE Trans. Control Syst. Technol.*, vol. 13, no. 6, pp. 911–920, 2005.

[5] V. Tsourapas, J. Sun, and A. Stefanopoulou, "Incremental step reference governor for load conditioning of hybrid fuel cell and gas turbine power plants," *American Control Conference*, pp. 2184–2189, June 2008.

[6] ——, "Incremental step reference governor for load conditioning of hybrid fuel cell and gas turbine power plants," *IEEE Trans. Control Syst. Technol.*, vol. 17, no. 4, pp. 756–767, July 2009.

[7] J. M. Elder, J. T. Boys, and J. L. Woodward, "Integral cycle control of stand-alone generators," *IEE Proc. C - Gener. Transm. Distrib.*, vol. 132, no. 2, pp. 57–66, 1985.

[8] D. Henderson, "An advanced electronic load governor for control of micro hydroelectric generation," *IEEE Trans. Energy Convers.*, vol. 13, no. 3, pp. 300–304, 1998.

[9] E. Gilbert, I. Kolmanovsky, and K. Tan, "Discrete-time reference governors and the nonlinear control of systems with state and control constraints," *Int. J. Robust Nonlin. Control*, vol. 5, pp. 487–504, 1995.

[10] A. Casavola and E. Mosca, "Reference governor for constrained uncertain linear systems subject to bounded input disturbances," *35th Conference on Decision and Control*, pp. 3531–3536, 1996.

[11] A. Bemporad, A. Casavola, and E. Mosca, "Nonlinear control of constrained linear systems via predictive reference management," *IEEE Trans. Autom. Control*, vol. 42, no. 3, pp. 340–349, 1997.

[12] E. G. Gilbert and I. Kolmanovsky, "Fast reference governors for systems with state and control constraints and disturbance inputs," *Int. J. Robust Nonlinear Control*, vol. 9, pp. 1117–1141, 1999.

[13] ——, "Set-point control of nonlinear systems with state and control constraints : a Lyapunov function reference governor approach," *38th Conference on Decision and Control*, pp. 2507–2512, 1999.

[14] E. Gilbert and I. Kolmanovsky, "Nonlinear tracking control in the presence of state and control constraints: a generalized reference governor," *Automatica*, vol. 38, no. 12, pp. 2063–2073, Dec. 2002.

[15] J. Willand, R.-G. Nieberding, G. Vent, and C. Enderle, "The knocking syndrome - its cure and its potential," *SAE Paper 982483*, 1998.

[16] N. Ravi, H.-h. Liao, A. F. Jungkunz, and J. C. Gerdes, "Modeling and control of exhaust recompression HCCI using split injection," *American Control Conference*, 2010.

[17] S. Jade, E. Hellström, A. Stefanopoulou, and L. Jiang, "On the influence of composition on the thermally-dominant recompression HCCI combustion dynamics," in *Dynamic Systems and Control Conference*, 2011.

[18] N. Ravi, H.-H. Liao, A. F. Jungkunz, and J. C. Gerdes, "Mid-ranging control of a multi-cylinder HCCI engine using split fuel injection and valve timings," *Sixth IFAC Symposium on Advances in Automotive Control*, 2010.

[19] B. Allison and A. Isaksson, "Design and performance of mid-ranging controllers," *J. Process Control*, vol. 8, no. 5-6, pp. 469–474, 1998.

[20] P. Gorzelic, E. Hellström, A. G. Stefanopoulou, and L. Jiang, "A coordinated approach for throttle and wastegate control in turbocharged spark ignition engines," 2012, accepted at the Chinese Control and Decision Conference.

[21] B. Allison and S. Ogawa, "Design and tuning of valve position controllers with industrial applications," *Trans. Inst. Meas. Control*, vol. 25, no. 1, pp. 3–16, Mar. 2003.

[22] J. Buckland, M. Jankovic, J. Grizzle, and J. Freudenberg, "Estimation of exhaust manifold pressure in turbocharged gasoline engines with variable valve timing," *Dynamic Systems and Control Conference*, 2008.

[23] A. Vahidi, I. Kolmanovsky, and A. Stefanopoulou, "Constraint management in fuel cells : a fast reference governor approach," *American Control Conference*, vol. 6, pp. 3865 – 3870, 2005.